# Structures of cyclotron lines in the presence of non-dipole magnetic field near the surface of neutron star

NISHIMURA Osamu*

We calculate the cyclotron lines in neutron star atmosphere assuming the surface magnetic field to be the superposition of the star-centered global dipole **d** and the crust-anchored dipole moment **m** which was modeled by Gil et al. We study how the crust-anchored dipole moment influences the properties of the cyclotron resonant scattering lines. When the extra dipole makes the magnetic field strength increase with altitude in the line-forming region, i.e. the sign of m is the minus, the structures of the cyclotron resonant scattering lines indicate broader line at the first harmonic and the ratio of the second to the first at the centroid energies of the cyclotron line is less than 2. This is consistent with the features observed in some X-ray pulsars. Thus, this may suggest that the strength of the magnetic field increases with the height of slab in line-forming region. In the atmosphere with the emission region in the middle of that, the cyclotron feature has only one emission line in either the redwing or bluewing due to the distribution of different strength of the magnetic field, although it has two emission lines in both the redwing and bluewing in an atmosphere threaded by an uniform magnetic field.

**keywords**: Cyclotron lines,atmospheres,magnetic fields

## 1. Introduction

Cyclotron lines in the spectra of neutron stars provide a powerful tool to measure directly the magnetic field strength of neutron stars. They have been observed in the spectra of more than 10 accretion-powered X-ray pulsars and indicate commonly broad and shallow features (Coburn et al. 2002). Makishima et al. (1999) point out that observed line widths are somewhat larger than those expected by thermal Doppler effects of the electrons. This probably suggests that other factors, which for example is the magnetic field variations and so on, contribute to the line widths.

The crust gives rise to small-scale anomalies which can be modeled by a number of crust-anchored dipoles oriented in different directions (Blandford et al. 1983; Arons 1993). Gil et al. (2002) considered the scenario where the magnetic field on the surface of a neutron star is non-dipolar assuming the presence of both the fossil field in the core and the crustal field structures. They modeled the actual surface magnetic field by superposition of the star-centered global dipole **d** and a crust-anchored dipole moment **m**, whose influence results in small-scale deviations of the surface magnetic field from the global dipole.

In the present paper, we employ Gil's (2002) model to investigate the influence of non-dipole magnetic field near the surface of neutron stars on the structures of the cyclotron lines. In one dimension, we solve the radiative transfer through the atmosphere near the surface of the neutron star with non-dipole magnetic field, which is obtained by calculating the star-centered global dipole field $\mathbf{B_d}$ plus a crust-anchored dipole field $\mathbf{B_m}$, $\mathbf{B_s} = \mathbf{B_d} + \mathbf{B_m}$.

The paper is organized as follows. In Section 2 we describe the surface magnetic field we employed. In Section 3, we present the spectra calculated by our model and discuss the effects of non-dipole magnetic field on the properties of cyclotron lines. we summarize our results and conclude in Section 4.

## 2. Surface magnetic field

According to Urpin et al. (1986), the magnetic field near the surface of neutron stars has non-dipolar component. The field configuration likely consists of a number of magnetic spots with typical size $\sim$ 100 m. Moreover, Gil & Mitra (2001) demonstrate that only the presence of strong non-dipolar surface magnetic field can favor such vacuum gap formation. We calculate the cyclotron lines in the atmosphere penetrated by the surface magnetic field which is calculated by using model proposed by Gil et al.(2002) Gil et al. (2002) modeled the actual surface magnetic field by superposition of the star-centered global magnetic dipole **d** and the crust-anchored local dipole moment **m**.

The resultant surface magnetic field is

$$\mathbf{B_s} = \mathbf{B_d} + \mathbf{B_m} \quad (1)$$

* Assistant Professor, Department of Electronics and Computer Science
Received May 20, 2005

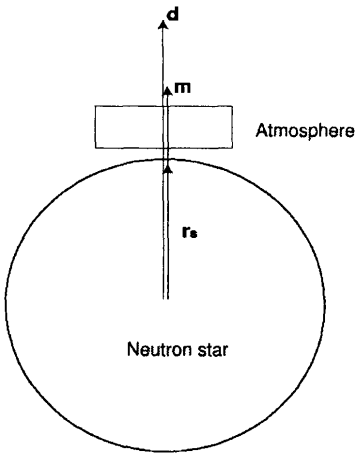


Figure 1 Schematic diagram of the atmosphere threaded by superposition of the star-centered global magnetic dipole "d" and crust-anchored local dipole "m" placed at $r_s$ in one dimension.

where

$$\mathbf{B_d} = (\frac{2\mathbf{d}cos\theta}{r^3}, \frac{\mathbf{d}sin\theta}{r^3}, 0) \quad (2)$$

and

$$\mathbf{B_m} = \frac{3(\mathbf{r}-\mathbf{r_s})(\mathbf{m}\cdot(\mathbf{r}-\mathbf{r_s})) - \mathbf{m}|\mathbf{r}-\mathbf{r_s}|^2}{|\mathbf{r}-\mathbf{r_s}|^5}, \quad (3)$$

where $\mathbf{r_s}$ is vector pointing the location of crust anchored dipole moment in considering the neutron star center as the origin. There are small-scale deviations of the surface magnetic field from the global dipole.

Gil et al.(2002) mostly consider an axially symmetric case in which both $\mathbf{d}$ and $\mathbf{m}$ are directed along the z-axis(parallel or antiparallel). Since we consider the magnetic field in one dimension as shown in Fig. 1, the global dipole and the crust anchored dipole magnetic field is respectively given by

$$B_d^r = \frac{2d}{r^3} \quad (4)$$

and

$$B_m^r = \frac{2m_r}{(r-r_s)^3}, \quad (5)$$

As a result, the resultant surface magnetic field is described by

$$B = B_d^r + B_m^r = \frac{2d}{r^3} + \frac{2m_r}{(r-r_s)^3}. \quad (6)$$

We calculate the X-ray spectra by solving radiative transfer through the atmosphere threaded by the magnetic field given by equation (6). The values of parameters $m$ and $r_s$ are assumed to be $\pm 1.2258 \times 10^{-4}$ and $0.95R$ in our works, respectively. Here, $R$ is the radius of neutron star which is assumed to be $10^6$ cm in the present paper.

We consider two cases of 1-0 geometry and 1-1 geometry for the boundary conditions( Isenberg et al. 1998). 1-0 geometry is the column depth between the source plane and the bottom of the slab is zero, i.e., a slab illuminated from below. 1-1 geometry is a slab with the source plane embedded in the middle of the slab. An initial injected photon distribution is assumed to be power-law.

## 3. Results

Within this simple model of a non-dipole surface magnetic field $\mathbf{B_s}$ one should expect that both cases $\mathbf{m}\cdot\mathbf{d} > 0$ and $\mathbf{m}\cdot\mathbf{d} < 0$ will occur with approximately equal probability. We investigate the properties of the cyclotron resonant scattering lines for both cases $\mathbf{m}\cdot\mathbf{d} > 0$ and $\mathbf{m}\cdot\mathbf{d} < 0$ in the 1-0 and 1-1 geometries. We assumed $m$ to be $\pm 1.2558 \times 10^{-4}$.

### 3–1 the sign of m is positive

**3–1–1 1-0 geometry** 1-0 geometry means that the photon source illuminates the line-forming region from below, which may correspond to a line-forming region in the magnetosphere of neutron star. Figure 2 shows the cyclotron lines formed through the atmosphere with the height of 100 m in 1-0 geometry. When the value of $m$ is positive, the features of the cyclotron lines are very similar to those which are obtained by assuming dipole magnetic field in the line-forming region (Nishimura 2003). The ratio of the centroid energies of the second harmonic line to the first therefore is more than 2. The emission lines at the blue wing are formed in the first harmonic lines due to photon spawning from resonant Raman scattering at higher harmonics in a different strength of the magnetic field, which is the superposition of the star-centered global dipole $\mathbf{d}$ and the crust-anchored dipole moment $\mathbf{m}$. Note that the cyclotron lines formed through the atmosphere threaded by non-dipole magnetic field show these features even in the cyclotron line-forming region with the height of about 100 m, while the width of the line-forming region is required to be more than about 500 m in the case of the atmosphere threaded by a dipole magnetic field.

In observation, two cyclotron absorption lines were also detected in the average spectrum of the high mass X-ray binary 4U 1907+09 observed

with the BeppoSAX satellite on 1997 September 27 and 28 (Cusumano et al.1998). They reported that the second line appears deeper than the first line. The ratio of the centroid energy of the second line with respect to the first line is also more than 2, in which two absorption features were detected at 18.8 keV and 39.4 keV respectively. This ratio may be attributed to the distribution of the magnetic field strength. According to Kreykenbohm et al. (1999), the ratio of the centroid energies seems to be also more than 2 in the accreting X-ray pulsar Vela X-1. They reported that the second harmonic line seems not to be coupled by a factor of 2 in centroid energy to the fundamental, but by a factor of 2.3 to 2.5 instead. In these X-ray pulsars, we can explain these ratios by considering either the extended atmosphere threaded by a dipole magnetic field or the small-scale atmosphere threaded by a non-dipole magnetic field which is generated by the superposition of the star-centered global dipole and the crust-anchored local dipole moment with a positive sign. The structures of the lines, however, are different from broad and shallow lines generally seen in the X-ray spectra observed in accretion-powered X-ray pulsars.

**3−1−2 1-1 geometry** 1-1 geometry means that the photon source is embedded in the line-forming region, which may correspond to a line-forming region on or near the surface of a neutron star in an accretion column. When the height of the atmosphere is 100m, the properties of the line features in the first harmonic significantly change. The emission features in the blueward wing are formed as in the case of 1-0 geometry, but become even stronger. This is due to emission feature formed in the source plane by line photons crossing the source plane many times. Moreover, this emission feature in the source plane is formed over the broad energy band corresponding to the various strengths of the magnetic field which exist in the line-forming region. After the formation of emission feature in the source plane, the absorption feature is formed in the upper atmosphere penetrated by the magnetic field weaker than that in the lower atmosphere. Consequently, strong asymmetry structures come to be formed in the first lines. The properties of the line features in the higher harmonics, however, do not significantly change, since the resonant scattering in the higher harmonics is nearly pure absorption due to resonant Raman scattering. When $m > 0$, the structures of the cyclotron lines in 1-1 geometry are relatively similar to those in 1-0 geometry.

It would be difficult to form the broad and shallow line feature at the first harmonic , as seen in observed X-ray spectra, in considering the atmosphere penetrated by the global dipole plus crust anchored dipole magnetic field with dipole moment $m > 0$, because photon spawning from resonant Raman scattering at the higher harmonics tends to convert the broad structures of the lines to one absorption plus one blueward emission-like feature.

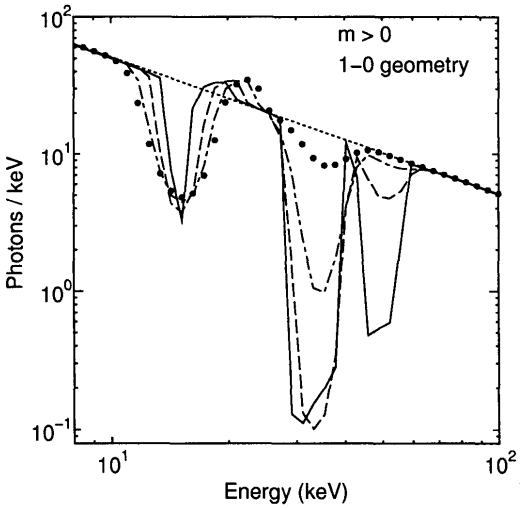


Figure 2 Spectra for slab thickness of $10^4$ cm, an electron number density of $N_e = 6.0 \times 10^{21}$ electron cm$^{-2}$, the temperature kT=5 keV, 1-0 geometry and the crust-anchored dipole moment $m > 0$. The solid, dashed, dot-dashed, thick-dotted curves represent spectra for $\mu = 0.1834, 0.5255, 0.7967$, and 0.9603, respectively. The dotted line denotes the power-law spectrum with $\alpha = 1$ emitted at the source plane.

### 3−2 the sign of m is negative

**3−2−1 1-0 geometry** When the sign of $m$ is negative, the features of the cyclotron lines in the first harmonic become very broad and shallow as shown in fig. 4. Moreover, the ratio of the centroid energies of the second harmonic line to the first is less than 2, which has actually been observed in 4U 0115+63 (Heindl et al. 1999), X0115+63 (Santangelo et al. 1999). Heindl et al. (1999) discovered a third harmonic CRSF in observations of outburst of 4U 0115+63 with the

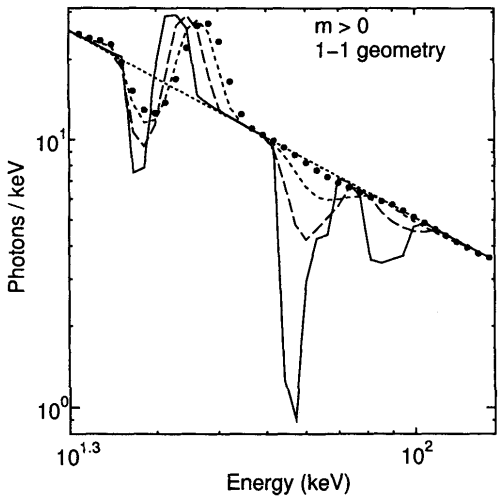


Figure 3 Same as figure 2, but for 1-1geometry.

RXTE. The spectrum in a narrow pulse phase range shows CRSFs at $12.40^{+0.65}_{-0.35}$, $21.45^{+0.25}_{-0.38}$, and $33.56^{+0.70}_{-0.90}$ keV. The CRSFs are not harmonically spaced with the centroid energy ratios to the fundamental of 1.73 ± 0.08 and 2.71 ± 0.13. They inferred that the second and third harmonics possibly originate at opposite poles, since the second and third harmonics are most significant in the main and secondary pulses, respectively.

Moreover, the four absorption-like features were observed in the spectrum of the recurrent hard pulsating X-ray transient X0115+63 with BeppoSAX (Santangelo et al. 1999). The ratios between the centroid energies of the lines with respect to the first are 1:(1.9):(2.8):(3.9). These ratios are significantly different from the classical values 1:2:3:4. They however pointed out that this result can be attributed entirely to the value of the centroid of the first harmonic, i.e., for a power-law plus cutoff model, the first harmonic would be at 12.79 ± 0.05 keV, while a fit to the other three harmonics gives a spacing of 12.02 ± 0.02 keV. The determination of its centroid energy could be responsible for a somewhat inadequate modeling of the continuum, since the first harmonic line is located close to the energy interval over which the slope of the X-ray spectrum steepens rapidly.

However, our models can explain these ratios assuming the presence of the crust-anchored local dipole moment with $m < 0$. This extra dipole moment with the minus sign would make the total magnetic field strength increase with altitude, so that the ratios between the centroid energies of the lines with respect to the first become smaller than the classical value. The reason is as follow: The first harmonic line is formed by resonant scattering, while the higher harmonic lines are formed by almost absorption process due to Raman scattering. The effect of scattering at the first harmonic make the peak of the absorption line generated in the upper atmosphere, since the transfer of photon in energy due to the effect of scattering buries the other part of the line core (Nishimura 2003). Consequently, the peak energy of the absorption line at the first harmonic tends to become the value corresponding to the stronger magnetic field than those of the absorption lines at the higher harmonics. Thus, the peak energy of only first harmonic line significantly deviates from the integer ratio in the centroid energies of the cyclotron lines due to the effect of scattering. As a result, the higher harmonic lines would almost show a harmonic relationship with a spacing of half of the centroid energy of the second harmonic line while the first harmonic line would not. The feature of this deviation is consistent with the results observed in some acrreting X-ray pulsars, such as X0115+63.

These features in the cyclotron lines could be formed when the magnetic field strength is inversely proportional to the distance from the emission region. The fact that the ratios between the centroid energies of the lines with respect to the first are less than integer value may therefore suggest that the strength of the magnetic field increases with altitude or horizontal direction.

**3−2−2 1-1 geometry** In 1-1 geometry, the structures of the first harmonic lines, which have one broad emission and absorption features, are different from one broad absorption line in the 1-0 geometry as shown in figure 5. In a slab threaded by a uniform magnetic field, the structures of the cyclotron lines at the first harmonic have two strong emission lines at both sides of an absorption line for 1-1 geometry. Consequently, the equivalent widths of absorption lines formed in 1-1 geometry are smaller than those formed in 1-0 geometry. First, we see that the structures of the first harmonic lines are much broader than those through the atmosphere threaded by the uniform magnetic field. Moreover, these have

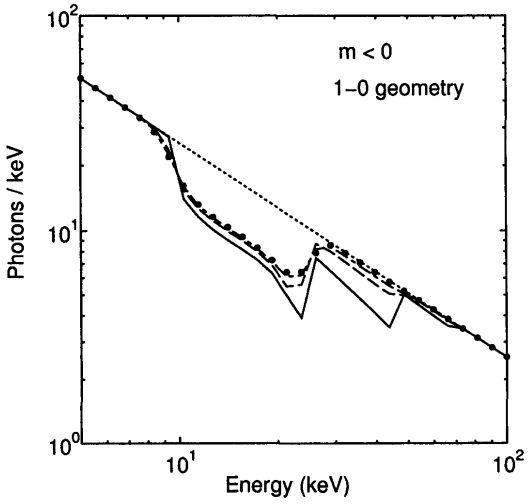


Figure 4 Spectra for slab thickness of 500 cm, an electron number density of $N_e = 3.0 \times 10^{20}$ electron cm$^{-2}$, the temperature kT=5 keV, 1-0 geometry and the crust-anchored dipole moment $m < 0$. The solid, dashed, dot-dashed, thick-dotted curves represent spectra for $\mu = 0.1834, 0.5255, 0.7967$, and 0.9603, respectively. The dotted line denotes the power-law spectrum with $\alpha = 1$ emitted at the source plane.

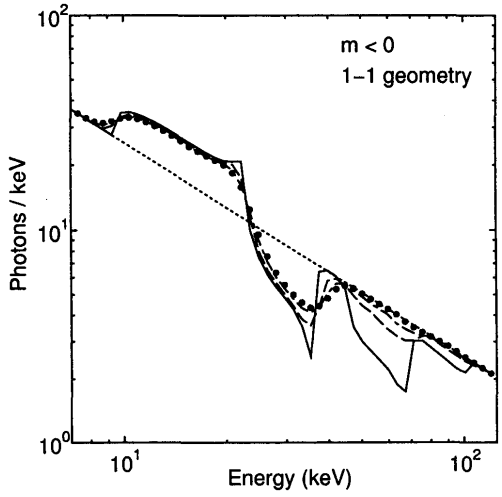


Figure 5 Spectra for slab thickness of $10^3$ cm, an electron number density of $N_e = 6.0 \times 10^{20}$ electron cm$^{-2}$, the temperature kT=5 keV, 1-1 geometry and the crust-anchored dipole moment $m < 0$. The solid, dashed, dot-dashed, thick-dotted curves represent spectra for $\mu = 0.1834, 0.5255, 0.7967$, and 0.9603, respectively. The dotted line denotes the power-law spectrum with $\alpha = 1$ emitted at the source plane.

the structures of shallow lines as observed in accreting X-ray pulsars, which were not able to be reproduced only by global dipole field (Nishimura 2003). Next, we see that the ratios of the centroid energies of the line at the second to the first are less than those in a slab threaded by a uniform magnetic field. The ratios of the peak energies of the higher harmonic absorption lines with respect to the first are 1:1.89:2.76, where the peak energies of the each harmonic absorption line indicate 36.1 keV, 68.2 keV, 99.7 keV, respectively. This is because the centroid energy in the first harmonic line corresponds to stronger magnetic field in the line-forming region than those in the higher harmonic lines. The centroid energy of the second harmonic line therefore corresponds to weaker strength of the magnetic field than that of the first in the same as 1-0 geometry. This result is consistent with the features of the ratios of the centroid energies observed in 4U 0115+63 (Heindl et al.1999) and X0115+63 (Santangelo et al. 1999).

The presence of the crust-anchored local dipole moment with the minus sign make these lines broader and shallower compared to the case of the crust-anchored local dipole moment with the positive sign. The reasons are as follow. In the case of dipole moment with the positive sign, photon spawning from resonant Raman scattering at the higher harmonics tends to produce an emission feature at blueward of an absorption line. Thus, broad structure of the absorption line is not formed in spite of the presence of different magnetic field strengths for the case of crust-anchored

local dipole moment with the positive sign.

## 4. Conclusions

We investigate the influence of non-dipole magnetic field on the structures of the cyclotron lines assuming the surface magnetic field to be superposition of the star-centered global dipole **d** and the crust-anchored dipole moment **m**. When $m > 0$, the properties of the cyclotron resonant scattering lines are similar to those formed through a slab threaded by a dipole magnetic field(Nishimura 2003). Cyclotron lines become broad and deep due to the intense strength variation of non-dipole magnetic field even for relatively thin slab $\sim 10^4$ cm. This result is not consistent with the cyclotron absorption features observed in accreting X-ray pulsars, since observed features are broad but shallow. When $m < 0$, the structures of the cyclotron resonant scattering lines in the first harmonic, however, are much broader and shallower than those in the case of $m > 0$ as shown in section 3. Our calculations show that the broad line structures could be formed for $m < 0$. In particular, the structures of the cyclotron lines calculated for 1-1 geometry and $m < 0$ are similar to those in pulse phase spectra of Her X-1 observed by HEAO 1 (Soong et al 1990), as shown in Fig. 9. Moreover, the ratios of the centroid energies of the line at the second to the first are less than those formed through a slab threaded by an uniform magnetic field. This result is consistent with the ratios of the centroid energies detected in observation of 4U 0115+63 with the RXTE(Heindl et al. 1999) and X0115+63 with BeppoSAX (Santangelo et al. 1999). This may suggest that the magnetic field strength in the line-forming region increases with the distance from the emission region.

In conclusion, the broad and shallow structures of the first harmonic lines and non-harmonicity in the ratios of the centroid energies of the line at the higher harmonics to the first in the cyclotron absorption lines in X-ray spectra of accreting X-ray pulsars may imply that magnetic fields in the line-forming region could have the structures such that the field strength increases with height or horizontal direction. The peak energy of the first harmonic absorption line shifts to redward of line center as $m > 0$ and blueward of line center as $m < 0$, since the cyclotron resonant process at the first harmonic is scattering. The peak energy of the second harmonic absorption line does not basically shift, since the opacity at the second harmonic does not depend on the strength of the magnetic field. The peak energy of the third harmonic absorption line shifts more or less to blueward of line center as both $m > 0$ and $m < 0$, since the opacity at the third harmonic depends on the strength of the magnetic field. Consequently, the peak energy of the third harmonic absorption line would tend to become higher than three times half of the centroid energy of the second harmonic. This result is consistent with feature detected in observation such as 4U 0115+63 (Heindl 2004 et al.).

I thank Q. Luo, D. Melrose and C. Zhang for careful reading of the manuscript and valuable discussions. I also would like to thank the University of Sydney for support and hospitality during my visit to the University. I acknowledge the Advanced Computing Center at RIKEN where the computations were done.

## 5. References

1) Arons, J. 1993, ApJ, 408, 160

2) Blandford, R. D., Applegate, J. H., & Hernquist, L. 1983, MNRAS, 204, 1025

3) Coburn, W., Heindl, W. A., Rothschild, R. E., Gruber, D. E., Kreykenbohm, I., Wilms, J., Kretschmar, P., & Staubert, R. 2002, ApJ, 580, 394

4) Cusumano, G., Di Salvo, T., Burderi, L., Orlandini, M., Piraino, S., Robba, N., & Santangelo, A. 1998, AAP, 338, L79

5) Gil, J., & Mitra, D. 2001, ApJ, 550, 383

6) Gil, J. A., Melikidze, G. I., & Mitra, D. 2002, AAP, 388, 235

7) Heindl, W. A., Coburn, W., Gruber, D. E., Pelling, M. R., Rothschild, R. E., Wilms, J., Pottschmidt, K. & Staubert, R. 1999, ApJ, 521, L49

8) Heindl, W. A., Rothschild, R. E., Coburn, W., Staubert, R. Wilms, J., Kreykenbohm I., Kretschmar P., 2004, astro-ph/0403197

9) Isenberg, M., Lamb, D. Q., & Wang, J. C. L. 1998, ApJ, 493, 154

10) Kreykenbohm, I., Kretschmar, P., Wilms, J., Staubert, R., Kendziorra, E., Gruber, D. E., Heindl, W. A., Rothschild, R. E. 1999, AAP, 341, 141

11) Makishima, K., Mihara, T., Nagase, F. & Tanaka Y. 1999, ApJ, 525, 978

12) Nishimura, O. 2003 PASJ, 55, 849

13) Santangelo, A. et al. 1999, ApJ, 523, L85

14) Soong, Y., Gruber, D. E., Peterson, L. E., & Rothschild, R. E. 1990 ApJ 348,641

15) Urpin, V. A., Levshakov, S. A., & Iakovlev, D. G. 1986, MNRAS, 219, 703